



SCHOOL OF PHYSICS

FINAL YEAR PROJECT REPORT

NAME:	Samuel A. Hopkins
DEGREE COURSE:	MSci Theoretical Physics
PROJECT TITLE:	Custom Project: Quantum Thermodynamics Related
YEAR OF SUBMISSION:	2023
SUPERVISOR:	Stephen R. Clark
NUMBER OF WORDS:	5569



Declaration

We produced all of the data presented in this project. Both partners produced code to contribute to the final results and obtained the same results with slightly differing implementations at times. All of the data produced was produced in python using methods from literature. Our supervisor helped us in the interpretation of our results, specifically how the entanglement entropy can saturate at a lower value in fermionic circuits. In terms of how work was divided between my partner and myself, we both wrote our respective programs to achieve the results, so that we may troubleshoot any issues faster. We both played an equal role in data collection, analysis and interpretation.

Acknowledgements

I'd like to thank Stephen Clark, for his enthusiastic attitude and continued guidance throughout the project.

Quantum Scrambling

Samuel A. Hopkins^{1*}

¹*H. H. Wills Physics Laboratory, University of Bristol, Bristol, BS8 1TL, UK**

(Dated: April 20, 2023)

Using atypical quantum circuit models, specifically super-Clifford and non-interacting fermion circuits, we explore the dynamics of operator space entanglement entropy and the process known as scrambling. In super-Clifford circuits, we reproduce the work from Blake and Linden, and achieve a maximal entanglement entropy using the stabilizer formalism. We find that no local operators can generate non-trivial entanglement dynamics within super-Clifford circuits. By using non-interacting fermion circuits we show that fermionic systems subject to random unitary circuits exhibit weak entangling dynamics in operator space, with its entanglement entropy saturating at a fraction of the Page value.

I. INTRODUCTION

Many-body systems and their dynamics play a central role in our understanding of modern physics with the dynamics of quantum many-body systems offering a great insight to a wide variety of fields in contemporary physics. Studying the evolution of quantum many-body systems presents challenging problems and has provided insightful results in condensed matter physics and quantum information [1]. Studying the dynamics of such systems is fundamentally a computational challenge due to the exponential growth of the Hilbert space with the number of qubits. However, quantum dynamics can be efficiently simulated in atypical quantum circuit models, providing a rich theoretical playground to test our understanding and uncover interesting phenomena. These atypical circuit models, known as classically simulable circuit models, will be analysed in hopes of understanding the spreading and scrambling of encoded local information, a process known as quantum scrambling. More precisely, quantum scrambling describes the process in which local information encoded by a simple product operator, such as a string of Pauli operators, becomes ‘scrambled’ by a amongst the large number of degrees of freedom in the system, such that, the operator becomes a highly complicated sum of product operators.

In recent years, the study of this scrambling process has seen immense research yielded new perspectives. These include new insights into the study of information in black holes and the AdS/CFT correspondence [2–5], quantum chaos, [6, 7] and operator hydrodynamics in many-body systems [8–11].

In order to investigate this phenomenon, classically simulable models provide excellent tools to gain a deeper understanding of operator evolution in hopes of applying any findings to generic cases of unitary evolution in many-body systems. As previously mentioned, some families of circuits are able to be efficiently simulated with polynomial effort on a classical computer. Two well-studied circuit models take the principal interest of this review, namely Clifford circuits and non-interacting fermion circuits. Clifford circuits and the Clifford group have played a key role in the study fault-tolerant quantum computing and, more recently, many-body physics via random Clifford unitaries [12, 13].

This is due to their efficient simulability on classical computers, despite the high amounts of entanglement that can be generated amongst states. Hence, circuits such as Clifford circuit are an ideal candidate in the study of many-body systems and their dynamics [14].

The second class of circuit models to be explored, are Matchgate or non-interacting fermion circuits. First introduced by Valiant [15] in the matchgate formalism and later identified with a physical model of non-interacting fermions in one dimension. This system has been shown to be classically simulable by DiVincenzo and Terhal [16] as an extension of Valiant’s findings. Thus, free fermion circuits form a good candidate to study scrambling phenomena, and the limitations of these circuit models.

* Email: cn19407@bristol.ac.uk
Supervisor: Stephen R. Clark
Word Count: 5569

With the use of recently developed techniques, the key objective of this project is to examine operator scrambling in models where the dynamics are analytically and numerically tractable. This is not possible in the generic unitary evolution of many-body systems due to an exponential growth of the Hilbert space with system size. However, by simulating the dynamics of scrambling in simulable circuit models, a picture of unitary evolution can be constructed, in hopes of gaining an understanding of dynamics of operator evolution and entanglement in atypical quantum systems.

II. QUANTUM INFORMATION AND COMPUTATION

A. Qubit Systems

1. Quantum Bits

In the theory of quantum computation, a quantum bit (qubit) is a spin- $\frac{1}{2}$ particle or a two-level system, in which a single bit of information can be encoded. Unlike its classical counterpart, where a bit occupies a binary state of 0 or 1, a qubit exists in a linear superposition of quantum states, expressed as $|\psi\rangle = \alpha|0\rangle + \beta|1\rangle$, where α and β are complex probability amplitudes that satisfy $|\alpha|^2 + |\beta|^2 = 1$. The states $|0\rangle$ and $|1\rangle$ form an orthonormal basis in the simplest Hilbert space, \mathbb{C}^2 , and are known as computational basis states. To extend this description to a system with 2 or more qubits, the use of the tensor product is required. For example, consider two subsystems A and B , with their respective Hilbert spaces, \mathcal{H}_A and \mathcal{H}_B such that they each describe a single qubit [17]. The total Hilbert space, \mathcal{H}_{AB} for the two-qubit, is constructed from \mathcal{H}_A and \mathcal{H}_B , as

$$\mathcal{H}_{AB} = \mathcal{H}_A \otimes \mathcal{H}_B. \quad (1)$$

To generalise, the Hilbert space of an n qubit system is written as,

$$\mathcal{H} = \mathcal{H}^{\otimes n} \equiv \mathcal{H}_1 \otimes \mathcal{H}_2 \otimes \cdots \otimes \mathcal{H}_n. \quad (2)$$

The many-qubit states that span \mathcal{H} are constructed identically, and are often expressed as a binary strings for a given configuration,

$$|x_1\rangle \otimes |x_2\rangle \otimes \cdots \otimes |x_n\rangle \equiv |x_1 x_2 \dots x_n\rangle. \quad (3)$$

2. Quantum Circuits

The overarching aim of this project focuses on the unitary evolution of quantum many-body systems, such as (2). The dynamics of such systems are described by the time-evolution operator, which maps an initial configuration, $|\psi_0\rangle$ to a time-evolved configuration $|\psi(t)\rangle$ as follows,

$$|\psi(t)\rangle = U|\psi_0\rangle. \quad (4)$$

Where U is an arbitrary matrix from the unitary group, $U(2^n)$, acting on the total Hilbert space and satisfying $UU^\dagger = U^\dagger U = I$. Conveniently, unitary evolution may be deconstructed into a sequence of linear transformations acting on finite subregions of the Hilbert space, represented as a quantum circuit. The quantum circuit is constructed to act on a set of qubits, called a register, with each time-step corresponding to a specific action by a quantum logic gate. This is analogous to classical computation, where circuits are comprised of logic gates acting on bit-strings of information. In contrast, quantum logic gates are linear operators that have a distinct matrix representation [18].

Each notable quantum logic gate has a specified gate symbol, as can be seen in Fig. 1, allowing the creation of complicated diagrammatic quantum circuitry that can be directly mapped to straightforward matrix manipulations for the simplest cases.

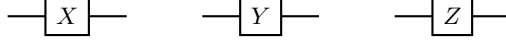


FIG. 1: Gate symbols for the Pauli operators in quantum circuits.

The gates shown in Fig. 1 are the Pauli operators, equivalent to the set of Pauli matrices, $P \equiv \{X, Y, Z\}$ which will also be denoted $(\{\sigma_x, \sigma_y, \sigma_z\})$ for which X, Y and Z are defined in their matrix representation as

$$X = \begin{bmatrix} 0 & 1 \\ 1 & 0 \end{bmatrix}, \quad Y = \begin{bmatrix} 0 & -i \\ i & 0 \end{bmatrix}, \quad Z = \begin{bmatrix} 1 & 0 \\ 0 & -1 \end{bmatrix}, \quad (5)$$

These gates are all one-qubit gates, as they only act upon a single qubit. Together with the Identity operator, I , the Pauli matrices form an algebra, satisfying the following relations:

$$XY = iZ, \quad YZ = iX, \quad ZX = iY, \quad (6)$$

$$YX = -iZ, \quad ZY = -iX, \quad XZ = -iY, \quad (7)$$

$$X^2 = Y^2 = Z^2 = I. \quad (8)$$

The set of Pauli matrices and the identity form the Pauli group, \mathcal{P}_n , defined as the 4^n n -qubit tensor products of the Pauli matrices (5) and the Identity matrix, I , with multiplicative factors, ± 1 and $\pm i$ to ensure a legitimate group is formed under multiplication. For clarity, consider the Pauli group on 1-qubit, \mathcal{P}_1 :

$$\mathcal{P}_1 \equiv \{\pm I, \pm iI, \pm X, \pm iX, \pm Y, \pm iY, \pm Z, \pm iZ\}. \quad (9)$$

From this, another group of interest can be defined, namely the Clifford group, \mathcal{C}_n , defined as a subset of unitary operators that normalise the Pauli group. Notable elements of this group are the Hadamard, Controlled-Not and Phase operators [19].

The Hadamard operator, H maps computational basis states to a superposition of computational basis states, written explicitly in it's action as,

$$H|0\rangle = \frac{|0\rangle + |1\rangle}{\sqrt{2}}, \quad H|1\rangle = \frac{|0\rangle - |1\rangle}{\sqrt{2}},$$

or in matrix form,

$$H = \frac{1}{\sqrt{2}} \begin{bmatrix} 1 & 1 \\ 1 & -1 \end{bmatrix}. \quad (10)$$

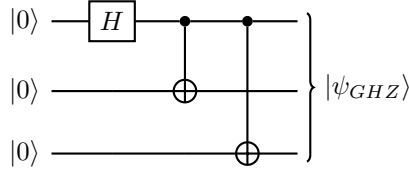
Controlled-NOT, $CNOT_{AB}$, is a controlled two-qubit gate. The first qubit, A acts as a 'control' for an operation to be performed on the target qubit, B . It's matrix representation is,

$$CNOT_{12} = \begin{bmatrix} 1 & 0 & 0 & 0 \\ 0 & 1 & 0 & 0 \\ 0 & 0 & 0 & 1 \\ 0 & 0 & 1 & 0 \end{bmatrix}$$

The Phase operator, denoted R is defined as,

$$R = \begin{bmatrix} 1 & 0 \\ 0 & e^{i\frac{\pi}{2}} \end{bmatrix}.$$

To give an example of a quantum circuit, consider the preparation of a GHZ state, $\frac{|000\rangle + |111\rangle}{\sqrt{2}}$ from an initial all-zero state, $|000\rangle$. This transformation may be drawn as,



Which is interpreted in operator form as,

$$|\psi_{GHZ}\rangle = (CNOT_{13})(CNOT_{12})(H \otimes I \otimes I)|000\rangle$$

III. FERMIONIC SYSTEMS

The familiar qubit system may be mapped onto a system of identical particles (fermions), such that the overall many body state describing the system, is invariant under particle exchange. This is performed via a Jordan-Wigner transformation, which maps any local spin-model to a local fermionic model [20]. To gain an understanding of how this can be carried out and why it is relevant, it will be useful to introduce the core concepts and language from *Second Quantization*.

1. Second Quantization and Indistinguishable Particles

The wave function for a system of N identical particles is $\psi(x_1, x_2, \dots, x_N)$, where a particle is specified by its position vector, \vec{x} . For bosonic systems, the wavefunction is symmetric under particle exchange, while fermionic systems present anti-symmetric wavefunctions under particle exchange called Slater determinants.

The construction of the n particle state via the extension of the single particle wavefunction, as described in (3), leads to a redundancy in its description of a many-body state and an unnecessarily large Hilbert space. A more efficient approach to describing many-body states is found in the formalism of second quantisation. Instead of describing states with Slater determinants, a *Fock state* presents an elegant and convenient basis in which to work in. The Fock state of a many-body system is represented in an occupancy number basis, written as $|n_1, n_2, \dots, n_L\rangle$, where n_i is the occupation number of a given local fermionic mode (LFM). For systems of bosonic particles, the occupancy can take any real non-negative integer. For systems of many fermionic particles, the occupancy number is either 0 or 1 with no two fermions ever occupying the same mode.

To preserve the symmetric properties of Fock states, second quantization introduces fermionic creation and annihilation operators. The creation operator, a_i^\dagger creates a particle at site i if unoccupied, and the annihilation operator, a_i , removes a particle at site i if occupied. More formally, its action on a Fock state may be written as,

$$a_j^\dagger |n_0, \dots, n_j, \dots, n_{m-1}\rangle = (-1)^{\sum_{s=0}^{j-1} n_s} (1 - n_j) |n_0, \dots, n_j - 1, \dots, n_{m-1}\rangle, \quad (11)$$

$$a_j |n_0, \dots, n_j, \dots, n_{m-1}\rangle = (-1)^{\sum_{s=0}^{j-1} n_s} n_j |n_0, \dots, n_j - 1, \dots, n_{m-1}\rangle. \quad (12)$$

With the fermionic creation and annihilation operators obeying crucial anti-commutation relations:

$$\{a_j, a_k\} \equiv \{a_j^\dagger, a_k^\dagger\} = 0, \quad \{a_j, a_k^\dagger\} = \delta_{jk} I. \quad (13)$$

Using these operators, an arbitrary Fock state, $|\psi_F\rangle$ of L modes, may be prepared from a set of creation operators acting on the vacuum, $|\Omega\rangle = |0, 0, \dots, 0\rangle$,

$$|\psi_f\rangle = (a_1^\dagger)^{n_1} (a_2^\dagger)^{n_2} \dots (a_L^\dagger)^{n_L} |\Omega\rangle. \quad (14)$$

2. Jordan-Wigner Transformation

Using the fermionic operators, the Jordan-Wigner transformation may be defined, which maps a system of N spin- $\frac{1}{2}$ particles onto a system of N ‘spinless’ fermions by defining the fermionic operators in terms of the Pauli spin operators [21],

$$a_i^\dagger = \left(\prod_{k=1}^{i-1} Z_k \right) \sigma_i^-, \quad a_i = \left(\prod_{k=1}^{i-1} Z_k \right) \sigma_i^+. \quad (15)$$

Where $\sigma_j^\pm = (X_j \pm iY_j)/2$. Such a mapping allows the Hilbert space of N qubits to be identified with the Hilbert space of N local fermionic modes (LFM’s). However this transformation is non-local, with fermionic operators having support over the almost the entire Hilbert space of N qubits [22].

As an alternative description, the *Majorana operators* may be defined as $c_{2k} = a_k + a_k^\dagger$ and $c_{2k+1} = i(a_k^\dagger - a_k)$ for $k = 1, \dots, N$ such that they satisfy $\{c_j, c_k\} = 2\delta_{jk}$. This description splits each LFM in two, increasing the number of modes to $2N$.

IV. SCRAMBLING DYNAMICS

A. Random Unitary Circuits

To study the generic quantum many-body systems, random unitary circuits provide a minimally structured model that can emulate the required dynamics of generic or ‘chaotic’ unitary evolutions.[14]. In the study of operator hydrodynamics The set-up is a chain of L spins, labelled as $q = 0, 1, \dots, L-1$ each with their respective local dimension h and is subject to a random unitary circuit \mathcal{U} . The total circuit is constructed per timestep, by acting with a layer of 2-qubit unitaries on evenly-bonded spins, followed by a layer of unitaries applied to odd-bonded spins. More formally, each timestep in the circuit corresponds to an action by $U = U_{\text{even}}U_{\text{odd}}$, where U_{even} is given by the tensor product of individual 2-qubit unitaries $U_{q,q+1}$ applied to all evenly bonded sites, $q, q+1$ for q even, and U_{odd} is given by the tensor product of individual 2-qubit unitaries $U_{q,q+1}$ applied to all odd bonded sites, $q, q+1$ for q odd. Each 2-qubit unitary acts on nearest neighbour spins, and is drawn from the uniform (Haar) probability distribution on the unitary group $U(4)$ or from a specific subgroup [23]. For our purposes, we require a simpler model. For a system of L qubits, each time step corresponds to a randomly drawn unitary acting on a randomly drawn qubit, q_i and it’s nearest neighbour, q_{i+1} .

To extract solvable dynamics and utilise well-established measures, information about the state of the system is encoded as strings of operators. A convenient basis to work with in qubit systems is found in the set of Pauli matrices. For example, a system with $L = 5$ spins could be represented by the operator string $\mathcal{O} = I \otimes I \otimes P_i \otimes I \otimes I$, where P_i is an arbitrary Pauli matrix. An operator of this form is a *local* operator, as it only acts non-trivially on a single site. For a system subject to generic unitary evolution, we expect that information encoded by an initially simple product operator to spread over the large number of degrees of freedom becoming highly complicated sum of global operators, such that they have support over the entire system. This process is known as Quantum Scrambling, and can be regarded as the combined notion of *Operator Spreading* and a growth in *Operator complexity*.

B. Operator Spreading

To give a picture of operator spreading, this section will primarily focus on the evolution of Pauli strings. Starting from some initially local product operator, such as $\mathcal{O} = \mathbb{1} \otimes \dots \otimes \mathbb{1} \otimes \sigma_x \otimes \mathbb{1} \otimes \dots \otimes \mathbb{1}$. This system will evolve via $|\psi(t)\rangle = U|\psi_0\rangle$ and the operator string will evolve via the Heisenberg evolution of operators,

$$\mathcal{O}(t) = U(t)\mathcal{O}U^\dagger(t). \quad (16)$$

Following this evolution, the local operator with minimal support, O_j has evolved to $O_j(t)$ with support over a large region of sites [8]. Operators that grow in this way, will spread ballistically [24–26] and are often characterised by

the out-of-time ordered correlator (OTOC) [27] and the square-commutator[28]. This also gives an intuitive picture of operator spreading, with the squared commutator defined as

$$C(t) = \langle [O(t), V_i][O(t), V_i]^\dagger \rangle \quad (17)$$

where V_i is a static local operator at site i [29]. Then at $t = 0$, $O(t)$ acts on a single site or a finite region of sites, such that it commutes with the static operator, V_i and $C(t) = 0$. Once the operator spreads, and becomes more non-local, the commutator increases as it's support overlaps with V_i .

C. Operator Complexity and Entanglement Entropy

A key component in quantum supremacy lies in a quantum algorithm's ability to utilise the abundant *entanglement* within a system. In simple bipartite systems, where $\mathcal{H}_{AB} = \mathcal{H}_A \otimes \mathcal{H}_B$, the state of this system, $|\Psi_{AB}\rangle \in \mathcal{H}_{AB}$ is said to be entangled if and only if the state cannot be written in product form, $|\Psi_{AB}\rangle = |\Psi_A\rangle \otimes |\Psi_B\rangle$, where $|\Psi_A\rangle$ and $|\Psi_B\rangle$ are the two vectors corresponding to the Hilbert spaces of each subsystem. If the state $|\Psi_{AB}\rangle$ is not entangled, then it is a product state and is said to be separable [30].

1. Entanglement In Qubit Systems

Qubit systems provide the simplest description of entangled states in bipartite systems. For a system of two qubits, there exist 4 specific maximally entangled configurations, called Bell states:

$$|\Phi^+\rangle = \frac{|00\rangle + |11\rangle}{\sqrt{2}}, \quad |\Phi^-\rangle = \frac{|00\rangle - |11\rangle}{\sqrt{2}}, \quad (18)$$

$$|\Psi^+\rangle = \frac{|01\rangle + |10\rangle}{\sqrt{2}}, \quad |\Psi^-\rangle = \frac{|01\rangle - |10\rangle}{\sqrt{2}}. \quad (19)$$

We can verify that the state, $|\Phi^+\rangle$ is an entangled state by writing,

$$|\Phi^+\rangle = [\alpha_0|0\rangle + \beta_0|1\rangle] \otimes [\alpha_1|0\rangle + \beta_1|1\rangle], \quad (20)$$

$$= \alpha_0\beta_0|00\rangle + \alpha_0\beta_1|01\rangle + \alpha_1\beta_0|10\rangle + \alpha_1\beta_1|11\rangle. \quad (21)$$

We require that the α_0 or β_1 terms must be zero in order to ensure the $|01\rangle$, $|10\rangle$ vanish. However, this would make the coefficients of the $|00\rangle$ or $|11\rangle$ terms zero, breaking the equality. Thus, $|\Phi^+\rangle$ cannot be written in product form and is said to be entangled.

2. Entanglement In Fermionic Systems

For a system of indistinguishable particles, each with only one spin degree of freedom (effectively spinless), entanglement can emerge as states analogous to a Bell state (18). Considering a system of 2 modes, occupied by a single indistinguishable particle, a fermion. The state of this system can be expressed as,

$$|\psi_f\rangle = \frac{|0_A\rangle|1_B\rangle - |1_A\rangle|0_B\rangle}{\sqrt{2}}. \quad (22)$$

Where A, B 'label' the two respective modes, and are included to express the state of this system intuitively. One can easily verify that this state is entangled, as outlined in (20), as it cannot be expressed in product form. However, this definition of entanglement is of little use when working with larger multi-fermion systems. We require entanglement measures to make qualitative statements on the complexity of operators and the systems they represent [31].

3. Entanglement Measures

For many-body systems, the definition of entanglement cannot be directly used to detect entanglement between states. Instead, entanglement measures provide a useful tool for detecting and analysing entanglement dynamics. In the case of distinguishable particles, one such entanglement measure is the *Schmidt Rank*, derived from the *Schmidt Decomposition*. The Schmidt decomposition states for any state vector, $|\Psi\rangle \in \mathcal{H}$ where $\mathcal{H} = \mathcal{H}_A \otimes \mathcal{H}_B$, there exists an orthonormal basis $\{|a_i\rangle \otimes |b_j\rangle\}$ such that,

$$|\Psi\rangle = \sum_{i=1}^{d_A} \sum_{j=1}^{d_B} D_{ij} |a_i\rangle \otimes |b_j\rangle. \quad (23)$$

Where d_A and d_B are the dimensions of the respective subsystems, A and B . The matrix D is a matrix of coefficients with the rank being the Schmidt rank. If the Schmidt rank is of rank one, then the state $|\Psi\rangle$ is a product state [30].

In systems of indistinguishable particles, a similar measure exists in the form of the *Slater Rank criterion*. The Slater Decomposition states that for a system of two fermions, in a N -dimensional space specified by the state vector,

$$|\Psi\rangle = \sum_{i,j=1}^N \omega_{ij} a_i^\dagger a_j^\dagger |\Omega\rangle. \quad (24)$$

There exists a unitary transformation, U that block diagonalises the coefficient matrix ω . More explicitly,

$$\omega' = U\omega U^T = \text{diag}[Z_0, Z_1, \dots, Z_r], \quad Z_i = \begin{bmatrix} 0 & z_i \\ -z_i & 0 \end{bmatrix}.$$

Where $z_i > 0 \forall i \in 1, \dots, r$ and Z_0 is an all-zero matrix of size $(N \times 2r) \times (N - 2r)$. The Slater rank is then the number of non-vanishing block matrices [32].

Entanglement measures such as the Schmidt and Slater rank, provide useful criterion for entanglement amongst state vectors. However, our aim is to analyse operator complexity signified by the entanglement in operator space. Thus, entanglement measures such as (23) and (24), do not provide the adequate tools to analyse the dynamics operator complexity in exactly solvable models. Instead we utilise an entropy entanglement measure, known as the Von Neumann entropy. For a quantum system described by the density matrix, ρ , the the Von Neumann entropy, S , is defined in general as,

$$S = -\text{Tr}(\rho \ln \rho). \quad (25)$$

To determine the entanglement entropy, a bipartition is introduced into the system, so that the entanglement entropy describes to which degree the two subsystems that have been partitioned are entangled. The entanglement entropy is then,

$$S_A = -\text{Tr}(\rho_A \ln \rho_A) = -\text{Tr}(\rho_B \ln \rho_B). \quad (26)$$

Where ρ_A , ρ_B describe the subsystems, A, B [33].

V. SIMULATING A QUANTUM CIRCUIT

The size of quantum systems presents computational challenges due to the exponential size of the Hilbert space. A system of L particles would have a 2^L dimensional Hilbert space. Simulating a quantum circuit of this size, requires the construction of this exponentially large Hilbert space, and since quantum dynamics typically utilize the full 2^L dimensional space, a classical computer can typically only simulate $L = 10 - 20$ particles in a given system. Thus, circuits that emulate quantum dynamics and can be simulated efficiently on a classical computer, provide immensely useful tools in the study of quantum systems. In one dimensional systems, there are three known classically simulable or exactly solvable models; Clifford circuits [34]; matchgates [35] or non-interacting fermion circuits [16]; and dual-unitary circuits [36]. We pin our focus on the first two, Clifford circuits and non-interacting or free fermion circuits.

A. Clifford Circuits

The main aim of a classically simulable circuit, is to reduce the total size of the system. Clifford circuits achieve this feat by abandoning the state-level description in favour of the operators that *stabilize* them. More explicitly, for an arbitrary quantum state vector, $|\psi\rangle$, this state is *stabilized* by an operator S if $|\psi\rangle$ is an eigenvector of S with eigenvalue 1: $S|\psi\rangle = |\psi\rangle$ [37]. Where S is an L qubit string of tensored Pauli operators. To simulate the time evolution of this system, only the Heisenberg evolution of stabilizers, $U(t)SU(t)^T \rightarrow S(t)$ needs to be simulated which can be achieved in polynomial time if $U(t)$ consists solely of gates from the Clifford group. This comes as a result of the structure of the Clifford group, as any product Pauli operator under conjugation by a Clifford unitary will always be mapped to another product of Pauli operators, by definition.

To implement this numerically, a $(L \times 2L)$ check matrix or stabilizer tableau is created, to encode the stabilizers and their dynamics. The stabilizer tableau, \mathcal{M} is constructed for L stabilizers, which act stabilize a state vector for L qubits, ordered as $q_1, \dots, q_i, \dots, q_L$. The i th row is constructed as follows: if the stabilizer S_i acts with the identity on the j th qubit, its value in the stabilizer tableau is 0. If S_i acts with σ_x , on the j th qubit, the $[i, j]$ value in \mathcal{M} is 1, if S_i acts with σ_y , on the j th qubit, the $[i, j]$ and $[i, j + L]$ values in \mathcal{M} are 1. If S_i acts with σ_z , on the j th qubit, the $[i, j + L]$ value in \mathcal{M} is 1. As an example, consider the Pauli string $\mathbb{1} \otimes \sigma_y \otimes \sigma_x \otimes \sigma_z$, which will be encoded in a stabilizer tableau as,

$$\mathbb{1} \otimes \sigma_y \otimes \sigma_x \otimes \sigma_z \rightarrow [0110|0101].$$

While Clifford circuits offer no constraint on the amount of entanglement within a system at a state-level description, we cannot expect the same for an operator-level description. Since gates from the Clifford group only map products of Pauli operators to products of Pauli operators, we can expect no operator complexity and hence no entanglement in operator space within Clifford circuits.

B. Blake and Linden's Construction

Blake and Linden [38] introduce a family of circuits that recover operator complexity on the space spanned by Pauli operators. They present a gate-set of 'super-Clifford operators' that generate a near-maximal amount of operator entanglement within the Pauli operator space, called super-Clifford circuits, when under time-evolution. These super-Clifford operators remain classically simulable, via an extension of stabilisers to operator space, called 'super-stabilisers'. Super-Clifford operators 'act' on Pauli operators, via conjugation in the Heisenberg picture. The first super-Clifford operator in the gate set is denoted as **Z.H**, which is identified with a on Pauli operators conjugation by a Phase gate, T :

$$T^\dagger XT = \frac{X - Y}{\sqrt{2}}, \quad T^\dagger YT = \frac{X + Y}{\sqrt{2}}. \quad (27)$$

Following this, the operators, X and Y can be changed to a state-like representation, with X denoted as $|\mathbf{0}\rangle$ and Y denoted as $|\mathbf{1}\rangle$. Then the action of **Z.H** can be written as,

$$\mathbf{Z.H}|\mathbf{0}\rangle = \frac{|\mathbf{0}\rangle - |\mathbf{1}\rangle}{\sqrt{2}}, \quad (28)$$

$$\mathbf{Z.H}|\mathbf{1}\rangle = \frac{|\mathbf{0}\rangle + |\mathbf{1}\rangle}{\sqrt{2}}. \quad (29)$$

The second gate in the set of super-Clifford operators, is the **SWAP** gate,

$$\mathbf{SWAP}|\mathbf{01}\rangle = |\mathbf{10}\rangle, \quad (30)$$

formed from the regular 2-qubit SWAP gate, that swaps two nearest neighbour qubits. It conjugates Pauli operators in the following way

$$\mathbf{SWAP}^\dagger X_1 Y_2 \mathbf{SWAP} = Y_1 X_2. \quad (31)$$

The third gate, denoted **C3**, acts as a combination of controlled-**Y** super-operators,

$$\mathbf{C3}[\mathbf{000}] = \mathbf{CY}_{12}\mathbf{CY}_{13}[\mathbf{000}] = [\mathbf{000}], \quad (32)$$

$$\mathbf{C3}[\mathbf{100}] = \mathbf{CY}_{12}\mathbf{CY}_{13}[\mathbf{100}] = -[\mathbf{111}]. \quad (33)$$

These three super-operators form the gate set $\{\mathbf{SWAP}, \mathbf{Z.H}, \mathbf{C3}\}$, which generates entanglement through unitary evolution in operator space, as this gate set maps Pauli strings to a linear superposition of Pauli strings. Despite the fact a simple string of Pauli operators can evolve into a sum of potentially exponential operator strings, the dynamics can be computed classically by extending the formalism of stabilizer states to operator space.

To calculate the entanglement entropy from the stabilizer tableau, a submatrix, \mathcal{M}_A must be formed by keeping the first $2p$ rows in \mathcal{M} , where p is the number of qubits in \mathcal{M}_A . The entanglement entropy is then given as,

$$S_A = I_A - p. \quad (34)$$

Where I_A is the rank of the submatrix \mathcal{M}_A .

Following this, Blake and Linden showed that the gate set was capable of generating near-maximal amounts of entanglement (slightly less than the Page value [39]) among Pauli strings on a chain of 120 qubits, quantified by the von Neumann entropy. This was only shown for operators with global support, and therefore shows no notion of operator spreading or entanglement growth in local operators.

C. Non-Interacting Fermion Circuits

The second class of classically simulable circuits first appeared as Matchgate circuits [15], which consist solely of 2-qubit gates, U_M , of the form,

$$U_M = \begin{pmatrix} p & 0 & 0 & q \\ 0 & w & x & 0 \\ 0 & y & z & 0 \\ r & 0 & 0 & s \end{pmatrix}, \quad U_M^1 = \begin{pmatrix} p & q \\ r & s \end{pmatrix}, \quad U_M^2 = \begin{pmatrix} w & x \\ y & z \end{pmatrix} \quad (35)$$

Where U_M^1, U_M^2 are elements of the special unitary group, $SU(2)$ and act on the even parity subspace ($\{|00\rangle, |11\rangle\}$) and the odd parity subspace ($\{|01\rangle, |10\rangle\}$). Systems that evolve via unitary evolution constructed from gates as in(35), are originally known as Matchgate circuits, and have been shown to be simulated efficiently on a classical computer [40]. Work by Terhal and DiVincenzo [16] related matchgate circuits to a model of non-interacting fermions in one dimension by mapping a system of n qubits, to a system of n local fermionic modes via the Jordan-Wigner transformation. This system is said to be *non-interacting*, if the Hamiltonian that mediates nearest-neighbour interactions is quadratic in the fermionic creation and annihilation operators.

1. A Fermionic Circuit

To preserve the number of fermions, such that elementary gates cannot create or annihilate on a fermionic mode, the circuit must act on the vacuum as, $U|\Omega\rangle = |\Omega\rangle$. Hence, a circuit that acts on L local fermionic modes, must consist solely of elementary gates $U = \exp(iH_g)$, where the gate Hamiltonian is written as,

$$H_g = \alpha_{ii}a_i^\dagger a_i + \alpha_{jj}a_j^\dagger a_j + \alpha_{ij}a_i^\dagger a_j + \alpha_{ij}^*a_j^\dagger a_i \quad (36)$$

The coefficients $\alpha_{ii}, \alpha_{jj}, \alpha_{ij}$ are considered to form an $L \times L$ matrix, α which is non-zero for the 2×2 subblock involving modes i and j . When expressed in matrix form as in(35), is of the form,

$$U_M = \begin{pmatrix} p & 0 & 0 & 0 \\ 0 & w & x & 0 \\ 0 & y & z & 0 \\ 0 & 0 & 0 & s \end{pmatrix}. \quad (37)$$

A circuit, U_C that is polynomial in the number of gates, acts on an arbitrary mode as,

$$U a_i^\dagger |\Omega\rangle = U a_i^\dagger U^\dagger U |\Omega\rangle = U a_i^\dagger U^\dagger |\Omega\rangle \quad (38)$$

To simulate this circuit, we switch to the alternative and more general description offered by Majorana fermions, c_i . An elementary gate in this description is of the form,

$$H_g = \frac{i}{4} \sum_{jk} \alpha_{jk} c_k c_l \quad (39)$$

Again, the coefficients α_{jk} form a $2 \times L \times 2 \times L$ matrix, which is non zero for a 4×4 subblock that mediates interactions between modes j and k . Then an elementary gate formed from acts by conjugations on mode j as

$$U c_j U^\dagger = \sum_k R_{jk} c_k \quad (40)$$

where R is a special orthogonal matrix, with determinant $+1$, ($R \in SO(2L)$). Then, the total circuit, is determined by the matrix multiplication of the rotation matrices constructed from each individual gate, reducing the system size from $2^L \times 2^L$ to $2L \times 2L$ in the number of qubits, L . Simulations of such a circuit require only polynomial effort and may be efficiently simulated given that the circuit, U , contains a polynomial number of gates.

2. Determination of the Rotation Matrices

To determine the rotation matrix from some initial gate Hamiltonian, these steps must be followed:

- I. Construct the $2L \times 2L$ real antisymmetric matrix, α is constructed from a given gate Hamiltonian.
- II. Block diagonalise α via the real Schur decomposition [41], which states for any real anti-symmetric matrix, there exists an orthogonal matrix W , such that,

$$W^T \alpha W = \begin{pmatrix} 0 & \lambda_1 & & \\ -\lambda & 0 & & \\ & & \ddots & \\ & & & 0 & \lambda_1 \\ & & & -\lambda & 0 \end{pmatrix} \quad (41)$$

Where $\pm\lambda$ are the eigenvalues of the matrix $i\alpha$.

- III. Construct the matrix, S from the eigenvalues of α :

$$S = \begin{pmatrix} \cos \lambda_1 & -\sin \lambda_1 & & \\ \sin \lambda_1 & \cos \lambda_1 & & \\ & & \ddots & \\ & & & \cos \lambda_L & -\sin \lambda_L \\ & & & \sin \lambda_L & \cos \lambda_L \end{pmatrix} \quad (42)$$

- IV. The rotation matrix, R , is then given by, $R = W^T S W$.

3. Correlation Matrices

To determine the entanglement entropy of a bipartite fermionic system, the correlation matrix, M needs to be constructed from the ground state. For two Majorana operators, c_j and c_k , the correlation matrix, M , is

$$M_{jk} \equiv \frac{i}{2} \langle \psi_{GS} | [c_j, c_k] | \psi_{GS} \rangle \quad (43)$$

Where $|\psi_{GS}\rangle$ is the ground state of the system and depends on the initial configuration of modes. By expressing the Majorana operators in terms of the canonical fermionic creation and annihilation operators, we can deduce the form of the correlation matrix from the action of these operators on a given Fock state. For a system with all modes unoccupied, $|\psi_{GS}\rangle$ is the vacuum state, $|\Omega\rangle$ and results in a correlation matrix of the form,

$$M^{\text{vac}} = \begin{pmatrix} -\sigma_z & & & \\ & -\sigma_z & & \\ & & \ddots & \\ & & & -\sigma_z \end{pmatrix} \quad (44)$$

Written concisely in terms of Pauli matrices and the $n \times n$ Identity matrix as, $M^{\text{vac}} = -(I_n \otimes \sigma_z)$. For a system with L modes occupied on every other site, e.g a Fock state of $|1, 0, 1, 0, \dots\rangle$, which we will call a half filled state, the correlation matrix takes the form,

$$M^{\text{half}} = \begin{pmatrix} \sigma_z & & & \\ & -\sigma_z & & \\ & & \sigma_z & \\ & & & \ddots \end{pmatrix} \quad (45)$$

For a system with L modes all occupied until the $L/2$ th mode, that corresponds to the initial fock state of $|1, \dots, 1, 0, \dots, 0\rangle$, which we will call the ‘Block’ state, the correlation matrix, M^{block} , takes the form,

$$M^{\text{block}} = \begin{pmatrix} \sigma_z & & & & \\ & \ddots & & & \\ & & \sigma_z & & \\ & & & -\sigma_z & \\ & & & & \ddots \\ & & & & & -\sigma_z \end{pmatrix} \quad (46)$$

The correlation matrix for an evolved system, $M = \langle U^\dagger c_j c_k U \rangle$ may be transformed via Eq. (40). Then to simulate a quantum circuit, we construct a correlation matrix to evolve via a random unitary circuit which has been transformed into a rotation matrix,

$$M_{ij} = \frac{i}{2} \langle \psi_{GS} | U^\dagger [c_j, c_k] U | \psi_{GS} \rangle \quad (47)$$

$$= \sum_{rs} R_{jr} R_{ks} \langle \psi_{GS} | [c_r, c_s] | \psi_{GS} \rangle. \quad (48)$$

4. Calculating the Entanglement Entropy

The entanglement entropy is computed from the correlation matrix, by taking the submatrix, M_A that bipartitions the system. Then M_A must be block-diagonalised, such that the eigenvalues, μ_i of the 2×2 blocks within M_A relate

to the eigenvalues, p_i , of the reduced density matrix (26) via,

$$p_i = \frac{|\mu_i| + 1}{2}. \quad (49)$$

The entanglement entropy may be calculated via the formula for the Shannon entropy,

$$S_A = \sum_i -p_i \log_2 p_i - (1 - p_i) \log_2 (1 - p_i). \quad (50)$$

5. Fermionic Gates

To create non-trivial gates from creation and annihilation operators, it is useful to look at specific mappings from states to some superposition of states. The non-interacting fermion circuits are constructed from the gates, $G(i, j)$ and $G(i, j, k)$. These are particle number conserving gates, such that they do not create or annihilate particles within the system and are of the form, (37). The action of $G(i, j)$ on two modes, can be expressed as,

$$\begin{aligned} G(i, j)|0, 1\rangle &\rightarrow |0, 1\rangle + |1, 0\rangle. \\ G(i, j)|1, 0\rangle &\rightarrow |1, 0\rangle + |0, 1\rangle. \end{aligned}$$

We restrict $G(i, j)$ to only act on nearest neighbour (n.n) modes, such that it can be expressed in terms of fermionic operators as,

$$G(i, i + 1) = \frac{\pi}{2} (a_i^\dagger a_i + a_{i+1}^\dagger a_{i+1} + a_i^\dagger a_{i+1} + a_{i+1}^\dagger a_i) \quad (51)$$

The 3-site gate, $G(i, j, k)$ is also restricted to only act on next nearest-neighbour modes. It's action can be expressed as,

$$\begin{aligned} G(i, j, k)|001\rangle &\rightarrow |001\rangle + |010\rangle + |100\rangle, \\ G(i, j, k)|010\rangle &\rightarrow |001\rangle + |010\rangle + |100\rangle, \\ G(i, j, k)|100\rangle &\rightarrow |001\rangle + |010\rangle + |100\rangle. \end{aligned}$$

In terms of fermionic operators(up to some coefficient),

$$\begin{aligned} G(i, i + 1, i + 2) &= a_i^\dagger a_i + a_{i+1}^\dagger a_{i+1} + a_{i+2}^\dagger a_{i+2} \\ &\quad + a_i^\dagger a_{i+1} + a_i^\dagger a_{i+2} + a_{i+1}^\dagger a_i \\ &\quad + a_{i+2}^\dagger a_i + a_{i+2}^\dagger a_{i+1} a_{i+1}^\dagger a_{i+2}. \end{aligned}$$

The fermionic swap gate from Bravyi and Kiteav [42] also served as a testbed for building the simulated circuit, but similar to the super-clifford circuits, it provided no entanglement within the system and is omitted from the simulations. For completeness, it's definition is given as,

$$SWAP_F = I - a_i^\dagger a_i - a_{i+1}^\dagger a_{i+1} + a_{i+1}^\dagger a_i + a_i^\dagger a_{i+1}. \quad (52)$$

VI. RESULTS

The first system to be investigated was the Stabilizer circuits constructed by Blake and Linden [38]. The system is encoded in an $N \times 2N$ matrix or stabilizer tableau, initialised for the all- X string, X_1, X_2, \dots, X_N . A random unitary circuit, constructed from the gates, **Z.H** and **C3**, for a circuit depth of $t = 20000$. The entanglement entropy is calculated at each time step via (refeq) and plotted against time to produce FIG. 2. The maximum entanglement

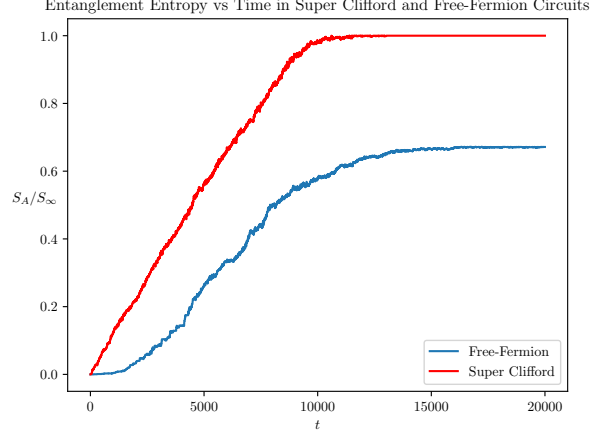


FIG. 2: Comparison of the operator entanglement entropy as a fraction of the maximum entanglement entropy S_∞ for a $N = 120$ qubit super-Clifford circuit and a $L = 120$ site, non-interacting fermion circuit. Clifford circuit is constructed from the **Z.H** and **C3** gates. The non-interacting fermion circuit is constructed from the $G(i, j)$ gate to act on an initially half filled state corresponding to M^{block} .

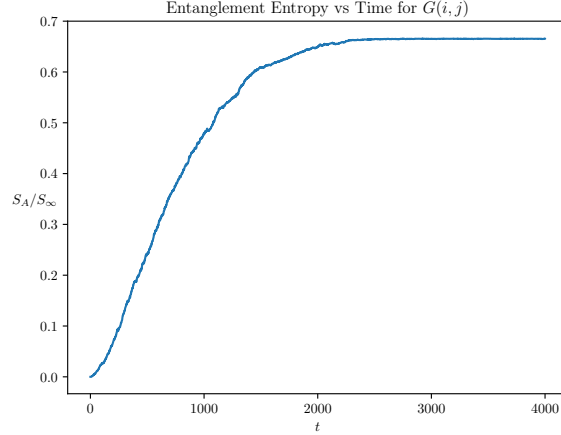


FIG. 3: Operator entanglement entropy as a fraction of the maximum entanglement entropy of a fermionic system with $L = 120$ modes subject to a non-interacting fermionic circuit of $G(i, j)$. Initial configuration of the system is the alternately-filled state corresponding to M^{half} .

entropy is found to saturate at the Page value [39], signalling a maximally entangled system. Note that the inclusion of **SWAP** does not affect any entanglement dynamics, and is omitted from the circuit. We also find that any intially local string of operators, e.g $I \dots X \dots I$ does not generate any entanglement within the system.

To compare with super Clifford circuits, systems of $L = 120$ modes were simulated for two configurations under two random unitary circuits, built from $G(i, j)$ and $G(i, j, k)$. Each gate was constructed in a simulation of the full state-level description, in order to verify the correct actions and expressions before using techniques to efficiently simulate the fermionic systems. Each circuit was first confirmed to not create entanglement on the vacuum state, corresponding to M^{vac} , and then subsequently simulated on the different filled configurations M^{half} and M^{block} . The results from the random unitary circuit built from $G(i, j)$ can be seen in Fig. 3 and 6. We find that for

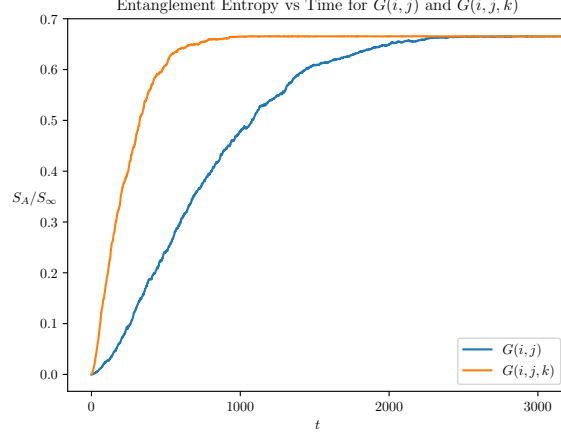


FIG. 4: Comparison of the operator entanglement entropy as a fraction of the maximum entanglement entropy of fermionic systems with $L = 120$ modes subject to non-interacting fermionic circuits of $G(i, j)$ and $G(i, j, k)$. Initial configuration of the system is the alternately-filled state corresponding to M^{half} .

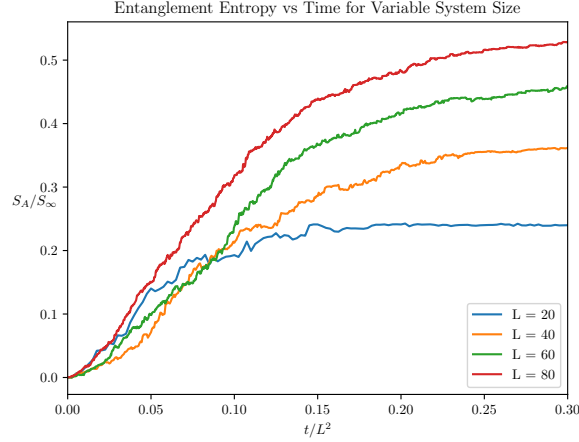


FIG. 5: Comparison of the operator entanglement entropy for fermionic systems of varying sizes, ($L = 20, 40, 60, 80$). L modes are subject to a random non-interacting fermionic circuits of $G(i, j)$ and $G(i, j, k)$. Initial configuration of the system is the alternately-filled state corresponding to M^{half} .

both system, the entanglement entropy does not saturate at the maximum Page value. The alternating half-filled state when subject to a random unitary circuit, saturates at $t \sim 2300$, which is considerably lower than the state corresponding to M^{block} , which saturates at $t \sim 16000$. This difference in saturation times, is concisely presented in Fig. 4, where saturation level is identical in both circuits, but the circuit built from $G(i, j)$ saturates significantly earlier. Simulations of varying system size were also carried out, and it can be seen that the entanglement saturation is directly dependent on the size of the system.

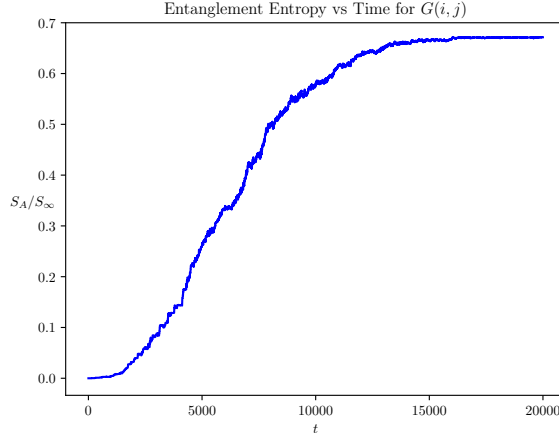


FIG. 6: Operator entanglement entropy as a fraction of the maximum entanglement entropy of a fermionic system with $L = 120$ modes subject to a non-interacting fermionic circuit of $G(i, j)$. Initial configuration of the system is the half-filled state corresponding to M^{Block} .

VII. DISCUSSION

A consistent theme within the entanglement entropy results for non-interacting fermion circuits, is systems of this nature, will not reach a maximally entangled state. We argue that this comes as a result of the heavily constrained set of gates, outlined in 37. Since this class of circuits can only be simulated using gates that are both non-interacting (no higher order terms) and particle number conserving, for the sake of operator complexity, we cannot expect a higher entanglement entropy saturation given that we immediately forbid an entire subspace, ($\{|00\rangle, |11\rangle\}$). In our circuit, if we start with a configuration in the odd parity subspace, ($\{|01\rangle, |10\rangle\}$), and only act on this subspace with particle conserving gates, then we can never enter into the even parity subspace and generate states, such as $|00\rangle$ and $|11\rangle$. This drastically reduces the number of given configurations of a time-evolved system and proposes an explanation as to how fermionic systems of this nature weakly entangle [43].

Another prominent feature in our fermionic circuits, is the rate of entanglement. Intuitively we would expect that longer range gates, and initial configurations that can generate fast scrambling, exhibit saturation at significantly lower timesteps than shorter range gates or more structured configurations. This is clearly shown in Fig. (4), where the random circuit constructed from $G(i, j, k)$, saturates at a lower timestep, t than the random circuit built from $G(i, j)$. In addition to this, for an initial Fock state configuration, such as $|1, \dots, 1, 0, \dots, 0\rangle$, it is expected that a significant time in the random circuit is spent generating no entanglement (you cannot mix or create superpositions from states such as $|111\rangle$). Instead, the random circuit has to slowly degrade the domain wall, or ‘surface’ of the fermionic state, i.e it has to create superpositions directly at the halfway modes, $|\dots, 1, 0, \dots\rangle$ in order to create entanglement.

Clifford circuits provided an intuitive introduction into exactly solvable circuit models. We successfully reproduced the results from Blake and Linden 2020 [38], with the exception of our circuit saturating at $t \sim 11000$ as opposed to Blake and Linden’s result of $t \sim 18000$. After correspondence with the author’s we determined that the circuit was extremely sensitive to initial configurations and conditions, but nevertheless exhibit identical properties and scaling of operator space entanglement entropy.

VIII. CONCLUSION

We have explored super Clifford and non-interacting fermion systems through the lens of operator complexity and quantum scrambling. We verify that the ‘super Clifford’ circuits constructed by Blake and Linden [38] generate

maximal entanglement entropy up to the Page value, in the space of operators with the $\{\mathbf{Z}, \mathbf{H}, \mathbf{C3}, \mathbf{SWAP}\}$ gate set and that initially local operators do not exhibit scrambling effects in super Clifford circuits.

In non-interacting fermion circuits, we find that fermionic systems weakly entangle and do not saturate the Page value, due to the restriction to particle number conserving gates. In addition to this, fermionic systems that generate high amounts of entanglement entropy require a large number of modes and that the saturation rate of entanglement entropy is highly dependent on the initial configuration and the range of gates being used.

An obvious extension to free-fermion circuits, is when the restriction of particle number conservation is lifted. However, this makes any interpretation of operator complexity increasingly difficult as it blurs the lines between the state-level and operator space descriptions. Nevertheless, it would be insightful to investigate methods to increase the saturation value of the operator space entanglement entropy in non-interacting fermion circuits. One proposed method is to change the geometry of the circuit being simulated via a random unitary circuit comprised only of fermionic SWAP gates. It is known and we have shown that SWAP gates do not affect the entanglement within systems directly, however we have also shown that the entanglement dynamics are sensitive to initial configurations. Such an extreme change to the initial configuration of the system may yield some interesting results.

Further directions into the study of quantum scrambling, may require new models and techniques. Tensor network methods have been shown to be extremely powerful in simulating one-dimensional quantum systems [44] and a more recently developed class of circuits, known as dual unitary circuits have been shown to be exactly solvable models of non-equilibrium physics[36].

-
- [1] A. Polkovnikov, K. Sengupta, A. Silva, and M. Vengalattore, “Nonequilibrium dynamics of closed interacting quantum systems,” *Reviews of Modern Physics*, vol. 83, pp. 863–883, aug 2011.
 - [2] P. Calabrese and J. Cardy, “Entanglement entropy and conformal field theory,” *Journal of Physics A: Mathematical and Theoretical*, vol. 42, p. 504005, dec 2009.
 - [3] K. Jensen, “Chaos in ads_2 holography,” *Physical Review Letters*, vol. 117, sep 2016.
 - [4] Y. Sekino and L. Susskind, “Fast scramblers,” *Journal of High Energy Physics*, vol. 2008, pp. 065–065, oct 2008.
 - [5] S. H. Shenker and D. Stanford, “Black holes and the butterfly effect,” *Journal of High Energy Physics*, 2014.
 - [6] J. Maldacena, S. H. Shenker, and D. Stanford, “A bound on chaos,” *Journal of High Energy Physics*, vol. 2016, aug 2016.
 - [7] S. H. Shenker and D. Stanford, “Stringy effects in scrambling,” 2014.
 - [8] V. Khemani, A. Vishwanath, and D. A. Huse, “Operator spreading and the emergence of dissipative hydrodynamics under unitary evolution with conservation laws,” *Physical Review X*, vol. 8, sep 2018.
 - [9] C. W. von Keyserlingk, T. Rakovszky, F. Pollmann, and S. L. Sondhi, “Operator hydrodynamics, otocs, and entanglement growth in systems without conservation laws,” *Phys. Rev. X*, vol. 8, p. 021013, Apr 2018.
 - [10] T. Rakovszky, F. Pollmann, and C. W. von Keyserlingk, “Diffusive hydrodynamics of out-of-time-ordered correlators with charge conservation,” *Phys. Rev. X*, vol. 8, p. 031058, Sep 2018.
 - [11] S. Grozdanov, K. Schalm, and V. Scopelliti, “Black hole scrambling from hydrodynamics,” *Physical Review Letters*, vol. 120, jun 2018.
 - [12] Y. Li, X. Chen, and M. P. A. Fisher, “Quantum zeno effect and the many-body entanglement transition,” *Phys. Rev. B*, vol. 98, p. 205136, Nov 2018.
 - [13] Y. Li, R. Vasseur, M. P. A. Fisher, and A. W. W. Ludwig, “Statistical mechanics model for clifford random tensor networks and monitored quantum circuits,” 2021.
 - [14] T. Farshi, J. Richter, D. Toniolo, A. Pal, and L. Masanes, “Absence of localization in two-dimensional clifford circuits,” 2022.
 - [15] L. G. Valiant, “Quantum computers that can be simulated classically in polynomial time,” in *STOC '01*, 2001.
 - [16] B. M. Terhal and D. P. Divincenzo, “Classical simulation of noninteracting-fermion quantum circuits,” tech. rep., 2001.
 - [17] B. Schumacher and M. Westmoreland, *Quantum Processes Systems, and Information*. Cambridge University Press, 2010.
 - [18] Any linear map between two finite dimensional vector spaces, in this case finite dimensional Hilbert spaces, may be represented as a matrix.
 - [19] M. A. Nielsen and I. L. Chuang, *Quantum Computation and Quantum Information: 10th Anniversary Edition*. Cambridge University Press, 2010.
 - [20] M. Lewenstein, A. Sanpera, and V. Ahufinger, *Ultracold Atoms in Optical Lattices: Simulating quantum many-body systems*. Oxford University Press, 03 2012.
 - [21] A. J. Landahl and B. C. A. Morrison, “Logical majorana fermions for fault-tolerant quantum simulation,” 2023.

- [22] M.-C. Bañuls, J. I. Cirac, and M. M. Wolf, “Entanglement in fermionic systems,” *Physical Review A*, vol. 76, aug 2007.
- [23] N. Hunter-Jones, “Operator growth in random quantum circuits with symmetry,” 2018.
- [24] D. A. Roberts, D. Stanford, and L. Susskind, “Localized shocks,” *Journal of High Energy Physics*, vol. 2015, mar 2015.
- [25] E. H. Lieb and D. W. Robinson, “The finite group velocity of quantum spin systems,” *Commun. Math. Phys.*, vol. 28, pp. 251–257, 1972.
- [26] T. Schuster and N. Y. Yao, “Operator growth in open quantum systems,” 2022.
- [27] S. Xu and B. Swingle, “Scrambling Dynamics and Out-of-Time Ordered Correlators in Quantum Many-Body Systems: a Tutorial,” feb 2022.
- [28] M. Blake, H. Lee, and H. Liu, “A quantum hydrodynamical description for scrambling and many-body chaos,” *Journal of High Energy Physics*, vol. 2018, oct 2018.
- [29] X. Chen and T. Zhou, “Operator scrambling and quantum chaos,” 2018.
- [30] R. Horodecki, P. Horodecki, M. Horodecki, and K. Horodecki, “Quantum entanglement,” *Reviews of Modern Physics*, vol. 81, pp. 865–942, jun 2009.
- [31] K. Eckert, J. Schliemann, D. Bruß, and M. Lewenstein, “Quantum correlations in systems of indistinguishable particles,” *Annals of Physics*, vol. 299, pp. 88–127, jul 2002.
- [32] J. Schliemann, J. I. Cirac, M. Kuś, M. Lewenstein, and D. Loss, “Quantum correlations in two-fermion systems,” *Physical Review A*, vol. 64, jul 2001.
- [33] B. Schumacher, “Quantum coding,” *Phys. Rev. A*, vol. 51, pp. 2738–2747, Apr 1995.
- [34] D. Gottesman, “The heisenberg representation of quantum computers,” 1998.
- [35] R. Jozsa and A. Miyake, “Matchgates and classical simulation of quantum circuits,” apr 2008.
- [36] R. Suzuki, K. Mitarai, and K. Fujii, “Computational power of one- and two-dimensional dual-unitary quantum circuits,” *Quantum*, vol. 6, p. 631, jan 2022.
- [37] D. Gottesman, “Stabilizer codes and quantum error correction,” 1997.
- [38] M. Blake and N. Linden, “Quantum circuits with classically simulable operator scrambling,” feb 2020.
- [39] D. N. Page, “Average entropy of a subsystem,” *Physical Review Letters*, vol. 71, pp. 1291–1294, aug 1993.
- [40] R. Jozsa and A. Miyake, “Matchgates and classical simulation of quantum circuits,” *Proceedings of the Royal Society A: Mathematical, Physical and Engineering Sciences*, vol. 464, pp. 3089–3106, jul 2008.
- [41] R. A. Horn and C. R. Johnson, *Matrix Analysis*. Cambridge University Press, 1985.
- [42] S. B. Bravyi, L. D. Landau, and A. Y. Kitaev, “Fermionic quantum computation,” tech. rep., 2000.
- [43] A more quantitative explanation may come in the form of a combinatorial argument on the given configurations of state vectors or density matrices, but this lies outside the time-scale of this project.
- [44] S. Xu and B. Swingle, “Accessing scrambling using matrix product operators,” *Nature Physics*, vol. 16, pp. 199–204, nov 2019.

Certification of ownership of the copyright

This Project Report is presented as part of, and in accordance with, the requirements for the degree of MSci/BSc (delete as applicable) at the University of Bristol, Faculty of Science.

I hereby assert that I own exclusive copyright in the item named below. I give permission to the University of Bristol Library to add this item to its stock and to make it available for consultation in the library, and for inter-library lending for use in another library. I also give consent for this report to be made available electronically to staff and students within the University of Bristol. It may be copied in full or in part for any bona fide library or research work. No quotation and no information derived from it may be published without the author's prior consent.

Author	Samuel Hopkins
Title	Custom Project: Quantum Thermodynamics related
Date of submission	20/04/23

I agree that submission of this report constitutes signing of this declaration.

This project/dissertation is the property of the University of Bristol and may only be used with due regard to the rights of the author. Bibliographical references may be noted, but no part may be copied for use or quotation in any published work without the prior permission of the author. In addition, due acknowledgement for any use must be made.